Published as: Sahnoune, M., Kaci, M., Taguet, A., et al. (2019). Tribological and mechanical properties of polyamide-11/halloysite nanotube nanocomposites. Journal of Polymer Engineering, 39(1), pp. 25-34. Retrieved 23 Dec. 2018, from doi:10.1515/polyeng-2018-0131

Tribological and Mechanical Properties of Polyamide-11/Halloysite Nanotubes Nanocomposites

Mohamed Sahnoune[1,2], Mustapha Kaci[1*], Aurélie Taguet[2], Karl Delbé[5], Samir Mouffok[4], Saïd Abdi[4] , José-Marie Lopez-Cuesta[2], Walter W. Focke[3]

[1]Laboratoire des Matériaux Polymères Avancés (LMPA), Université de Bejaia, 06000, Algeria
[2]Centre des Matériaux des Mines d'Alès (C2MA), IMT Mines d'Alès, 6 avenue de Clavières, 30319 Alès cedex, France
[3]Institute of Applied Materials, University of Pretoria, South Africa
[4]Laboratoire des Sciences et Génie des Matériaux, Faculté de Génie Mécanique et Génie des Procédés, USTHB. Alger
[5]Laboratoire de Génie Production (LGP), ENIT-INPT, Université de Toulouse, 47 Avenue d'Azereix, Tarnes, France
[*] Corresponding author: < kacimu@yahoo.fr>

Abstract

This article reports some morphological, tribological, and mechanical data on polyamide-11(PA11)/halloysite nanotube (HNT) nanocomposites prepared by melt-compounding. HNTs extracted from the Djebel Debbagh deposit in Algeria were incorporated into the polymer at 1, 3, and 5 wt%. For comparison, commercial HNTs were also used under the same processing conditions. Scanning electron microscopy showed that both HNTs were homogeneously dispersed in the PA11 matrix, despite the presence of few aggregates, in particular at higher filler contents. The tribological properties were significantly improved, resulting in a decrease in the friction coefficient and the wear rate characteristics due to the lubricating effect of HNTs. This is consistent with optical profilometry data, which evidenced the impact of both types of HNTs on the surface topography of the nanocomposite samples, in which the main wear process was plastic deformation. Furthermore, Young's modulus and tensile strength were observed to increase with the filler content, but to the detriment of elongation at break and impact strength. Regarding the whole data, the raw Algerian halloysite led to interesting results in PA11 nanocomposites, thus revealing its potential in polymer engineering nanotechnology.

Key words: halloysite; mechanical properties; optical profilometry; polyamide-11; tribology

1. Introduction

Polyamide-11 (PA11) is a versatile thermoplastic polymer exhibiting excellent characteristics in terms of abrasion and chemical resistance, piezoelectric and ferroelectric properties or resistance to heat [1]. Moreover, PA11 is biocompatible and has the advantage to be less hydrophilic than the commonly used polyamide-6 and 6,6 [2,3].Therefore, PA11 is widely used as engineering polymer in a wide range of industrial fields, from automotive to offshore applications, including food packaging. Indeed, polyamides, especially PA6 and PA6,6, are widely used as a replacement for bronze, brass, aluminum or steel parts as wear materials [5] due to their hardness, strength, and tribological properties [4]. However, PA11 has poor wear resistance [4], which can limits its application in the offshore or automotive fields, with wear being the most important constituent of tribology [6]. In order to improve the tribological properties of polyamides, several methods have been reviewed with as main challenge the reduction of wear and friction rates in order to save and reduce the energy while increasing the productivity[6]. One of the most promising approach is the nanocomposite technology, where recent investigations on the influence of different nanofiller particles in polyamides, have shown a considerable improvement in tribological properties even at low filler content [4,7–9].Nevertheless, the mechanism which describes the nanoparticles effect in enhancing the wear resistance of polymers remains still in debate[10]. One explanation for the wear behavior of nanocomposites can be related to the high contact surface area of the nanofiller, which favors the interactions polymer-filler[11].

Recently, halloysite nanotubes (HNTs)have attracted significant attention as a new type of nanofiller for polymer nanocomposites in relation to those most commonly used, i.e. montmorillonite clays and carbon nanotubes (CNTs)[12].HNTs have a higher intrinsic stiffness

compared to the montmorillonite nanoplatelets [13,14]. They are inexpensive, naturally available and biocompatible[15]. In addition, HNTs do not require exfoliation due to their unique tubular structure with few hydroxyl groups on the surface. HNTs are minerals of the kaolin group with the following chemical composition:$Al_2Si_2O_5(OH)_4.nH_2O$.Various polymer/HNTs nanocomposite systems were investigated using different matrices based on polymer thermoplastics [13,16–20], thermosets [21–24] and elastomers [25,26]. The main results arising from these studies indicated an enhancement of tensile properties such as Young's modulus and tensile strength, thermal stability and fire retardancy.PA11/HNTs system has not been investigated extensively and only a few publications can be found in the open literature [1,27,28]. Prashantha *et al.*[27] reported that addition of HNTs to PA11 realizes a tailor-made material with multifunctional characteristics, while in recent papers, the Algerian HNTs were successfully used both as reinforcing agent and compatibilizer in various polymer blends : PA11/PS [29], PA11/SEBS-g-MA [30]or PHBV/PBS[31].

In this work, we aimed to investigate the tribological and mechanical properties of PA11nanocomposites filled with raw Algerian halloysite prepared by melt mixing at filler contents of 1, 3 and 5 wt%. The results will be discussed on the basis of those obtained with a commercial halloysite and neat PA11.

2. Experimental

2.1. Materials

PA11 (Rilsan® LMNO) was supplied by Arkema(France). According to the manufacturer, this grade is free of additives. The weight average molecular weight = 51000 g/mol with a density of 1.02 g/cm^3.Algerian halloysite nanotubes (referenced as HNTs A) were extracted from Djebel Debbagh deposit in Guelma (Algeria). The filler particles have an average diameter of 25 µm and a surface area of 51.4 m^2/g. **Fig.1** shows a TEM micrograph of

raw Algerian halloysite nanotubes. For further details, see ref. [31]. Prior to use, the stone-like raw HNTs A were finely ground into powder using a laboratory mill and sifted through a 40 µm sieve to obtain particles having an average diameter of 25 µm. A commercial halloysite (referenced as HNTs C) was purchased from Sigma Aldrich (France) and used for comparison purpose. The main characteristics of HNTs Care as follows: outer diameter= 30-70 nm,length = 1.3 µm, density = 2.53 g/cm^3,surface area = 64 m^2/g and CEC= 8 meq/g. Prior to processing, HNTs and PA11 were dried under vacuum at 80°C for 24 h and overnight, respectively, to remove moisture traces.

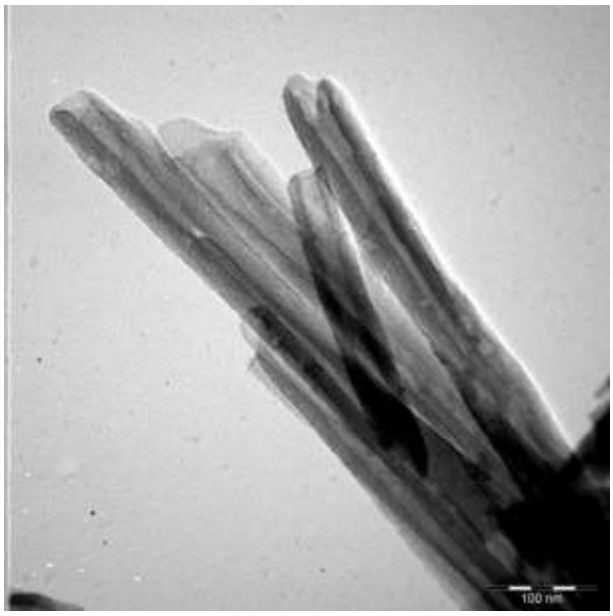

Fig 1.TEM micrograph of Algerian halloysite nanotubes.

2.2. Sample preparation

Various PA11/HNTs nanocomposite samples filled at 1, 3 and 5wt% were prepared by melt compounding under vacuum in a semi-industrial twin-screw extruder (BC 21 Clextral) having a screw diameter (Φ) = 25 mm and length to diameter ratio (L/Φ) = 48 at a screw speed of 250 rpm according to the compositions reported in **Table 1**.The temperature profile was 140/230/235/245/250 °C from the hopper to the die. After pelletizing, the granules were dried under vacuum at 80°C overnight and then injection molded into standard test specimens for

tribological and mechanical tests using an injection-molding machine KM50-180X (Krauss Maffei). The temperature profile ranged from 220 to 225 °C and the mold temperature was kept at 40 °C. Holding pressure and screw rotation speed were 135 bar and 100 rpm, respectively, with a throughput of 50 cm^3/s.

Table 1. Codes and composition of the samples.

Sample	PA11 (wt%)	HNTs A (wt%)	HNTs C (wt%)
PA11	100	0	0
PA11/H1	99	1	0
PA11/H3	97	3	0
PA11/H5	95	5	0
PA11/HC1	99	0	1
PA11/HC3	97	0	3
PA11/HC5	95	0	5

2.3. Characterization

2.3.1. Scanning electron microscopy (SEM)

SEM was conducted under high vacuum with an environmental SEM Quanta 200 FEG (FEI Company) operating at 12.5 kV. SEM was used to evaluate the degree of dispersion of HNTs in PA11 matrix. Specimens obtained by injection molding were cryo-fractured and coated with a thin carbon layer and the fracture surfaces were observed in the back-scattered electrons (BSE) mode. Moreover, the fracture surface of the samples after Charpy test as well as the worn surfaces after being sputter-coated with a silver gold film were also observed.

2.3.2. Tribological measurements

Tribological tests were carried out on a CSM pin-on-disk tribometer according to ASTM G99-05 standard procedure. An assembly diagram of the friction pairs is shown in **Fig.2**. A spherical ended pin is placed in contact with the sample surface (disc) under a predetermined load, which generates a friction force. 6 mm diameter hardened steel ball was involved as the counter body. All the sliding tests were performed under ambient conditions with a normal load of 10 N at a sliding speed of 0.3 m/s and a sliding distance of 800 m. The wear track radius considered was 6 mm. Before the test, the surface roughness of the samples (Ra) was determined using a piezoelectric transducer roughness meter (TR100). The surfaces were cleaned and thoroughly dried to remove all dirt and foreign matter.

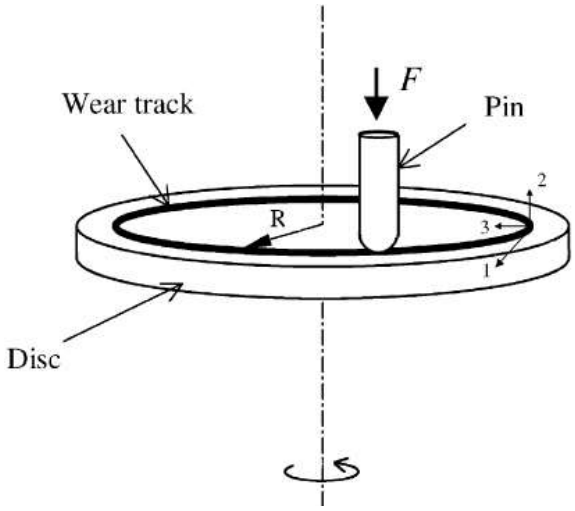

Fig 2. Schematic diagram of the friction pairs in the pin on disc tribometer.

During sliding, the friction coefficient was continuously measured and recorded in real time by the tribometercomputer software (TriboX) and the average value is given. The average values of friction coefficient in the test range were used as the friction coefficient of samples [32].The wear rate (*W)* (mm^3/N.m) of each specimen was calculated using Equation 1.

$$W = V_{disk}/FD_s \text{(Equation 1)}$$

Wher e*F* is the load used, *Ds* the sliding distance and V_{disk}, the disc volume loss which is given by Equation 2.

$$V_{disk} = 2\pi R[r^2\, sin^{-1}\left(\frac{d}{2r}\right) - \left(\frac{d}{4}\right)(4r^2 - d^2)^{1/2}] \text{(Equation 2)}$$

Where *R* is the wear track radius, *d* the wear track width and *r*, the pin end radius.

The wear track width (*d)* was determined using an optical microscope (Nikon) and image analysis software. At least four measurements were recorded for each sample at different representative locations in the track and the average values were reported.

2.3.3. Tensile test

Stress-strain analysis was evaluated from ISO 527-2 IA type tensile bars according to ISO 527 standard test procedure. Young's modulus was accurately measured using an extensometer clip-on incremental (ZwickRoell) at a cross-head speed of 1 mm/min, whereas yield strength and elongation at break were determined at a speed of 20 mm/min. The measurements were carried out with a tensile machine Zwick Z010 (ZwickRoell) at environmental conditions. Prior to testing, the samples were stored at 23 °C and 50% RH for 10 days, according to ISO 527 standard. At least ten specimens of each formulation were tested and the average values were reported.

2.3.4. Charpy impact

Notched Charpy impact strength of the samples was determined using a Zwick 5102 pendulum impact tester (ZwickRoell) according the ISO 179 standard test procedure. The notched specimens had the following dimensions:80×10×4 mm^3 and a depth notch of 2.0 mm. Prior to testing, all specimens were stored as dry as molded at 23 °C and 0% RH for 10 days. At least ten specimens of each formulation were tested and the average values were reported.

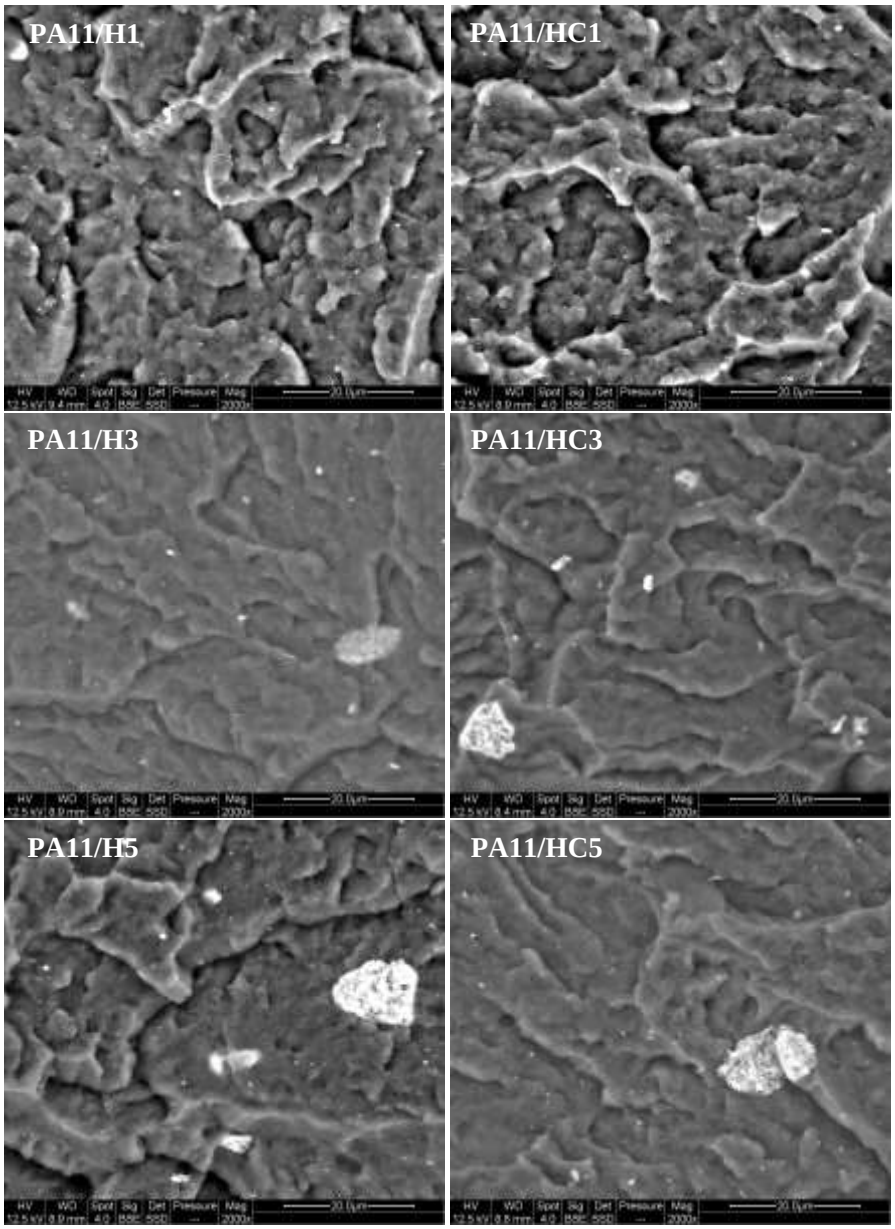

Fig.3. SEM micrographs of fractured surfaces of the PA11/HNTs samples.

3. Results and discussion

3.1. Morphology

SEM micrographs offractured surface of differentPA11/halloysite nanocomposites samples are shown in **Fig.3**. The images reveal a homogeneous and uniform dispersion of both raw and commercial halloysite particles in the PA11matrixmost of the nanotubes being

dispersed at the nanoscale. However, a few aggregates, which seem to increase with increasing the filler content irrespective to the type of halloysite, are also visible but they are less than 15 µm in size. These aggregates for HNTs A correspond to the micronic particles resulting from the comminution process of raw halloysite. However, the presence of agglomerates in the case of HNTs C is quite surprising, regarding the high purity of the commercial clay. This suggests that at higher HNTs content, the intensity of the mixing process and the filler-matrix interactions were insufficient to facilitate complete break-up of the pre-existing HNTs aggregates. The fine dispersion of halloysite particles in PA11 matrix may be the result of good affinity between the two components.

3.2. Tribological properties

The surface roughness values (Ra) of neat PA11and PA11/HNTs nanocomposites measured before sliding test are reported in **Table 2**. The obtained results reveal values of Ra forthe different samples ranged between 0.26 and 0.35 µm. The values are very small and are conform to the ASTM G99-05 standard procedure, which recommends surface roughness values less than 0.8 µm. The results confirm also the good preparation procedure of the samples and the good adherence of the nanoparticles to the matrix.

Table 2. Surface roughness (Ra), average friction coefficient (μ) and Wear rate (*W*) of neat PA11 and PA11/HNTs nanocomposites.

Sample	Surface roughness(Ra) (μm)	Average Friction coefficient (μ)	Wear rate (*W*) (10^{-5} mm^3/N.m)
PA11	0.32	0.43± 0.02	8.6
PA11/H1	0.28	0.39± 0.02	5.7
PA11/H3	0.3	0.35± 0.03	4.4
PA11/H5	0.35	0.35± 0.02	4.6
PA11/HC1	0.32	0.40± 0.02	6.5
PA11/HC3	0.26	0.37± 0.02	5.3
PA11/HC5	0.31	0.39± 0.02	5.6

One of the most important characteristics of the tribology is the friction coefficient. In this regard, **Fig.4 (a)** and **(b)** shows the evolution of the friction coefficient of the neat PA11 and the different nanocomposite samples as a function of sliding distance for HNTs A and HNTs C, respectively. The whole curves exhibit two different stages, i.e. initial and steady state stages. In the first stage, which is also called running-in period, the friction coefficient increases from a static value to the highest one characterizing the initial step of the friction process. In the second stage starting from around 70 m, the friction coefficient remains almost unchanged along the sliding distance. According to the data reported in **Table 2**, the addition of HNTsdecreases slightly the friction coefficient of PA11, being maximum at 3 wt% filler content. Indeed, the values of the friction coefficient of PA11 nanocomposite samples filled with the Algerian halloysite are reduced by about 9% at 1 wt%, while at 3 and 5 wt%,

19%decrease is noted. Similar trend is observed for PA11/HNTsC nanocomposites, however less pronounced than those filled with HNTsA.

(a)

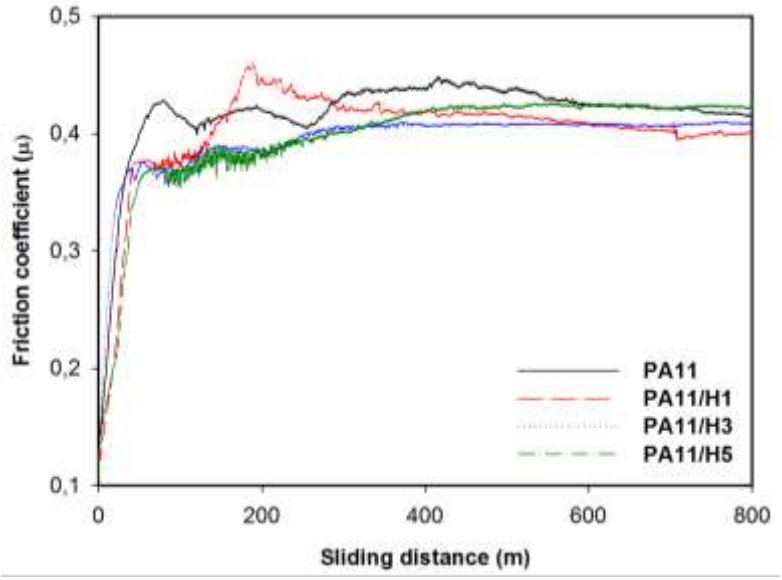

(b)

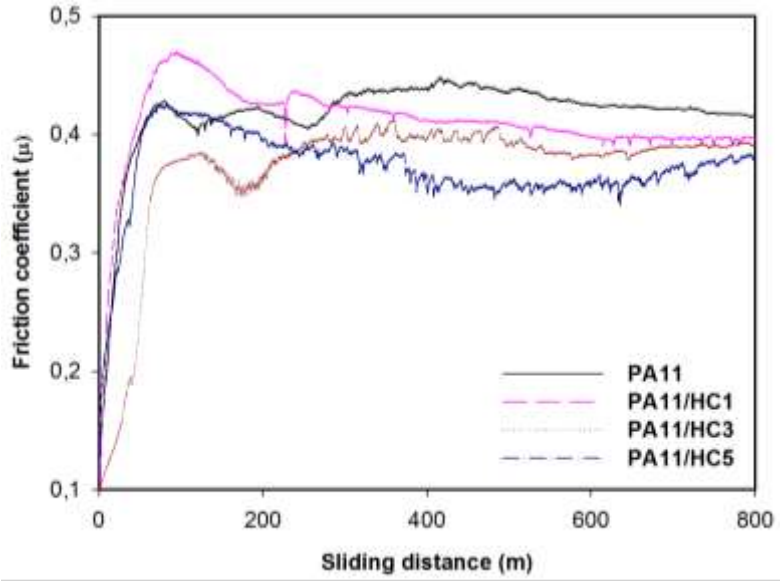

Fig.4. Evolution of the friction coefficient (μ) of the samples as a function of the sliding distance. Nanocomposites filled with HNTs A (a) and HNTs C (b).

The improved tribological properties of PA11/HNTs were also investigated through the determination of the wear rate (*W*) and the main results are summarized in **Table 2**. As well

known, any enhancement in the tribological properties requires a reduction of the wear rate. The wear track width after sliding tests is illustrated in **Fig.5**. From **Table 2**, it appears clearly that the addition of HNTs decreases significantly the wear rate of PA11with an optimum filler rate of 3 wt%. The incorporation of 1 and 3 wt% of HNTs A reduces *W* of PA11 from 8.610^{-5} to 5.710^{-5} and 4.410^{-5} mm^3/N.m, corresponding to a decrease of 33.7 and 48.8%, respectively. At 5 wt%, the wear rate of the PA11/H5sampleincreases slightly but still remains below that of neat PA11. For the PA11 nanocomposites filled with HNTs C, similar trend is also noticed with the commercial halloysite, however less pronounced than the PA11/ HNTsA ones.

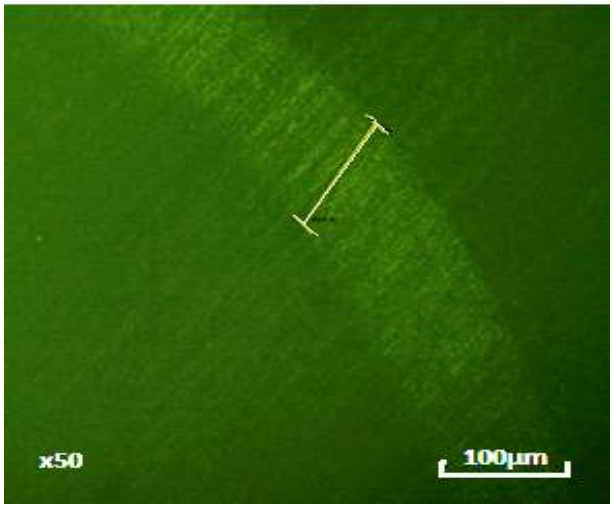

Fig.5. Wear track width after sliding tests.

According to the literature [7,8,32–34], the wear rate decrease is interpreted as a result of the formation of a tenacious transfer layer on the counter face by the nanoparticles, which protects the composite surface from direct contact with the counter face, reducing thereby, the friction and wear of the nanocomposite samples. Whereas, the phenomenon observed at 5 wt% may be attributed to the formation of HNTs agglomerates as observed in **Fig.3**. Consequently,the material becomes more easily peeled off during sliding processing [35]. Moreover, at higher filler content, crystallinity of the nanocomposite materials is reduced, leading to higher friction coefficient and wear rate[9].

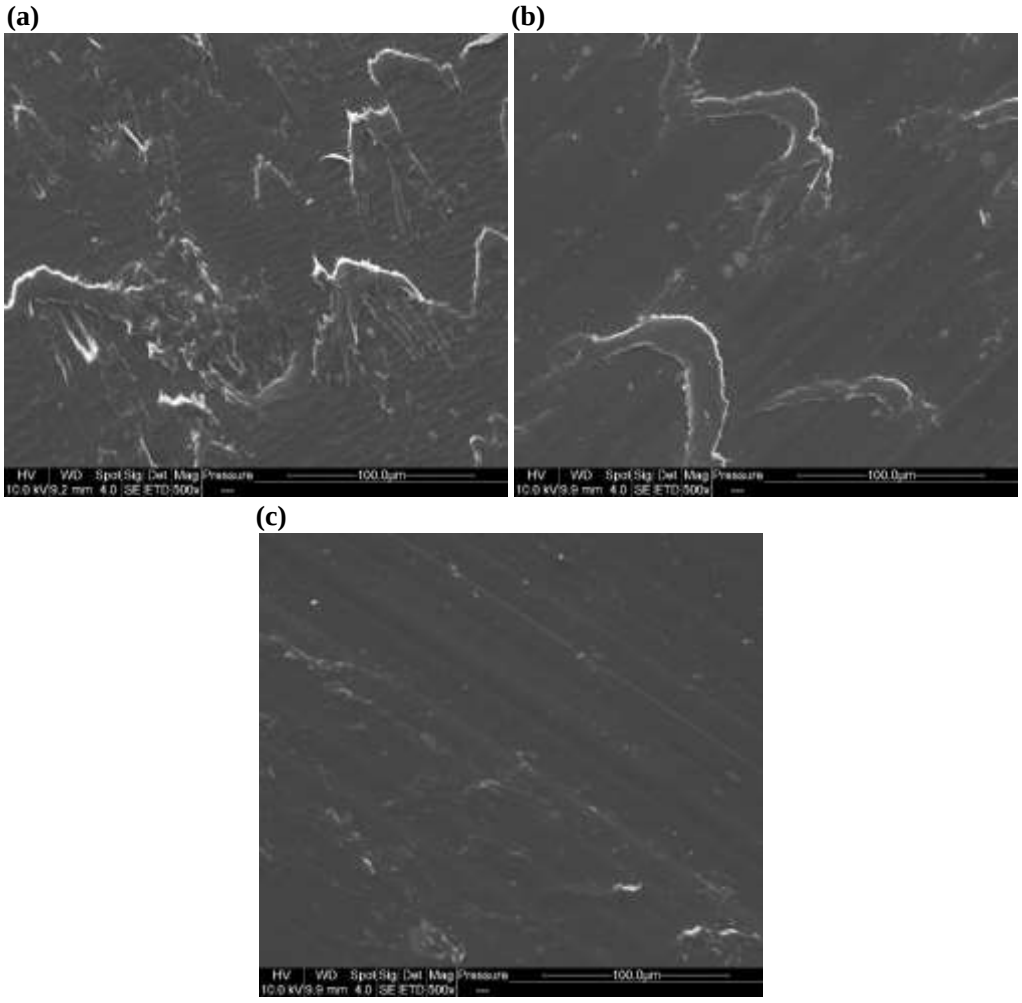

Fig.6. SEM micrographs of the worn surfaces during testing under a load of 10 N and at a sliding speed of 0.3 m/s of PA11 **(a)**, PA11/H5 **(b)** and PA11/HC5 **(c)**.

Fig. 6 shows the worn surfaces of the neat PA11 and those of PA11/H5 and PA11/HC5 nanocomposites. From **Fig.6 (a)**, it can be seen that the matrix shows a rough surface with significant damages and the presence of some lumps. This suggests that the wear process is governed by plastic deformation and adhesive wear mechanism [9]. Whereas, in **Fig.6 (b)** relative toPA11/H5 sample, the worn surface reveals traces of shallow micro cutting and wear-particle accumulation. This is due probably to the presence of an excessive amount of halloysite particles in the sample (5 wt%),causing a tilting of the adhesive wear towards an abrasive wear, impacting negatively both the mechanical strength and shear deformation of the nanocomposite

surface. Unlike the nanocomposite filled with the commercial halloysite, i.e.PA11/HC5 (**Fig.6 (c)**), which see the shearing surface considerably reduced. Indeed, a smoother surface is observed with reduced wear particles accumulation. The results are in accordance with the tribological measurements, which evidenced the action of halloysite clay through the reduction of the friction coefficient and the wear rate.

Table 3. Main mechanicals properties of neat PA11 and PA11/HNTs nanocomposites obtained by tensile and notched Charpy tests.

Sample	Young's Modulus (GPa)	Tensile strength (MPa)	Elongation at break (%)	Impact strength (KJ/m^2)
PA11	1219.9 ± 54.9	41.2 ± 0.6	228.1 ± 14.2	5.5 ± 0.3
PA11/H1	1390.3 ± 55.5	44.6 ± 0.3	160.8 ± 15.6	3.8 ± 0.4
PA11/H3	1411.1 ± 32.1	43.8 ± 0.3	115 ± 27	3.9 ± 0.2
PA11/H5	1511.2± 75.4	44.6± 0.3	94.2± 15.6	3.6 ± 0.2
PA11/HC1	1348.2 ± 47.9	43.6 ± 0.9	224.6 ± 60.5	4.3 ± 0.7
PA11/HC3	1411.1 ± 35.1	43.9 ± 0.7	129 ± 53.8	3.2 ± 0.4
PA11/HC5	1463.5 ± 55.3	43.5 ± 0.3	100.6 ± 38.4	3.1 ± 0.6

3.3. Mechanical properties

Both tensile and impact strength values of neat PA11 and PA11/HNTs nanocomposites are provided in **Table 3**. As expected, the incorporation of 5 wt% of HNTs Ain PA11induces an increase in Young's modulus of the nanocomposite sample by24% compared to the neat polymer. This is attributed to the reinforcing effect of the clay filler and it is consistent with the literature data [1,13,36–38]. On the other hand, the elongation at break of PA11/H5decreasesby

58% compared to neat PA11, while its impact strength is reduced by 34%.Similar trend is also observed with HNTs C in PA11 nanocomposites, however the effect is less pronounced than the Algerian halloysite. Indeed, the Young's modulus value of PA11/HC5 only increases by 20%, while its impact strength decreases by almost 44% compared with the neat PA11.

According to the literature [14], an improvement of mechanical properties of the nanocomposite materials depends on the degree of dispersion of the filler in the polymer matrix together with filler-filler and filler-polymer matrix interactions. Therefore, the enhancement of tensile strength of the nanocomposites is only due to the intrinsic stiffness of the individually dispersed halloysite nanotubes [13]. Regarding toughness, halloysite nanotubes can play a double role, i.e.in the first instance the HNTs can enhance the toughness via a crack-bridging effect [13,36], while in the second scenario, halloysite aggregates can cause stress concentrations in the sample, increasing its brittleness.

In order to gain a better understanding on the mechanical behavior effect of halloysite on PA11, SEM micrographs of the fractured surface of PA11 loaded at 5 wt% with both HNTs A and HNTs C after undergoing the notched Charpy impact test are shown in **Fig.7 (a)**and**(b)**, respectively. Both figures show a good interfacial adhesion between halloysite nanotubes and PA11matrix, confirming thus the surface roughness results (**Table 2**). Moreover, most of HNTs particles are well imbedded in the polymer matrix even if some pulled out nanotubes are observed.

(a)

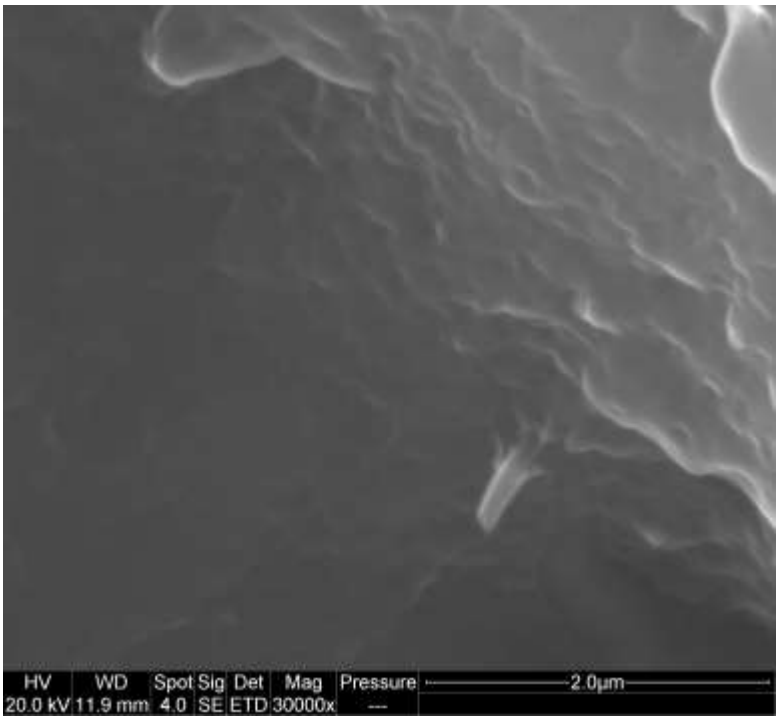

(b)

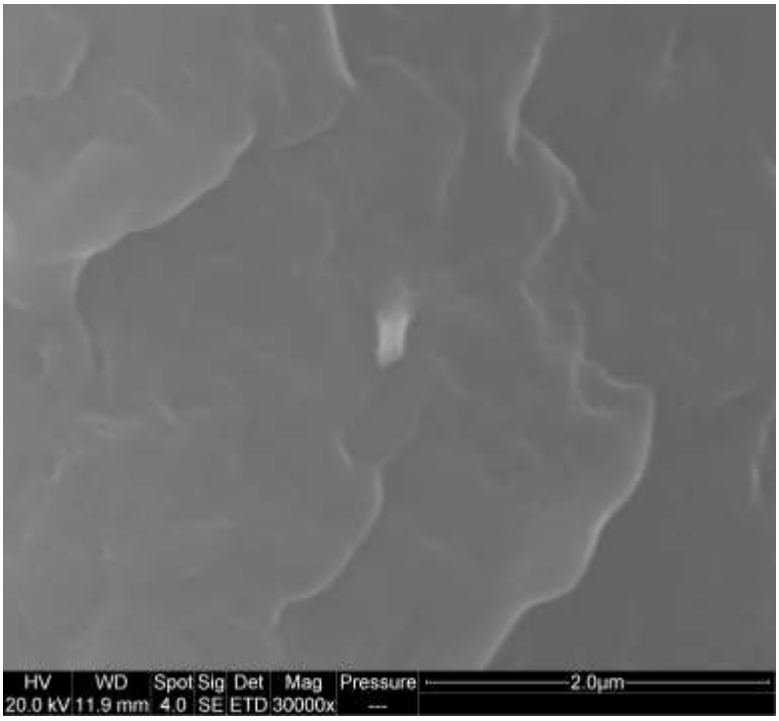

Fig.7. SEM micrographs of fractured surfaces of PA11/H5 **(a)** and PA11/HC5 **(b)** after undergoing notched Charpy test.

4. Conclusions

The study focused on the use of crude Algerian halloysite as nanofiller in PA11 matrix in order to improve the tribological and mechanical performances of the nanocomposite materials prepared by melt mixing. The data obtained were compared to those obtained with commercially pure available halloysite. The SEM analysis of PA11/HNTs nanocomposites morphology showed a regular dispersion of HNTs in PA11 even though the formation of filler aggregates was evident, especially at higher content ratio. The addition of both halloysite nanotubes to PA11 improved its tribological properties by reducing both the friction coefficient and wear rate parameters, however the effect was more pronounced for the nanocomposite samples filled with the Algerian halloysite. Furthermore, 3 wt% appeared to be the optimum filler ratio. Moreover, the mechanical data indicated a reinforcement effect of HNTs in PA11 nanocomposites with however, a relative loss of toughness. The whole results led to the conclusion that the use of raw Algerian halloysite is promising in the elaboration of PA11 nanocomposites since no prior treatment is necessary. It has the potential to compete with the commercial ones as reinforcement agent to improve tribological and mechanical performances of PA11.

Acknowledgments

The authors are grateful to EGIDE for its financial support through the Tassili program 13MDU891, to Jean-Jacques Flat from Arkema and the Algerian CompanySOALKA for supplying PA11 resin and raw Algerian halloysite, respectively. The authors are also thankful to Benjamin Gallard for his help for the elaboration of the nanocomposite samples.

References

[1] Hao A, Wong I, Wu H, Lisco B, Ong B, Sallean A, et al. Mechanical, thermal, and flame-retardant performance of polyamide 11–halloysite nanotube nanocomposites. J Mater Sci 2015;50:157–67.

[2] He X, Yang J, Zhu L, Wang B, Sun G, Lv P, et al. Morphology and melt rheology of nylon 11/clay nanocomposites. J Appl Polym Sci 2006;102:542–9.

[3] Liu T, Lim KP, Tjiu WC, Pramoda KP, Chen ZK. Preparation and characterization of nylon 11/organoclay nanocomposites. Polymer 2003;44:3529–35.

[4] Ambrósio JD, Balarim CVM, de Carvalho GB. Preparation, characterization, and mechanical/tribological properties of polyamide 11/Titanium dioxide nanocomposites. Polym Compos 2016;37:1415–24.

[5] Samyn P. Large-scale specimen testing on friction and wear of pure and internally lubricated cast polyamides. Tribotest 2006;12:237–56.

[6] Giraldo LF, López BL, Brostow W. Effect of the type of carbon nanotubes on tribological properties of polyamide 6. Polym Eng Sci 2009;49:896–902.

[7] Srinath G, Gnanamoorthy R. Effect of nanoclay reinforcement on tensile and tribo behaviour of Nylon 6. J Mater Sci 2005;40:2897–901.

[8] Dasari A, Yu Z-Z, Mai Y-W, Hu G-H, Varlet J. Clay exfoliation and organic modification on wear of nylon 6 nanocomposites processed by different routes. Compos Sci Technol 2005;65:2314–28.

[9] Li Y, Ma Y, Xie B, Cao S, Wu Z. Dry friction and wear behavior of flame-sprayed polyamide1010/n-SiO2 composite coatings. Wear 2007;262:1232–8.

[10] Bahadur S. The development of transfer layers and their role in polymer tribology. Wear 2000;245:92–9.

[11] Burris DL, Boesl B, Bourne GR, Sawyer WG. Polymeric Nanocomposites for

Tribological Applications. Macromol Mater Eng 2007;292:387–402.

[12] Liu M, Jia Z, Jia D, Zhou C. Recent advance in research on halloysite nanotubes-polymer nanocomposite. Prog Polym Sci 2014;39:1498–525.

[13] Hedicke-Höchstötter K, Lim GT, Altstädt V. Novel polyamide nanocomposites based on silicate nanotubes of the mineral halloysite. Compos Sci Technol 2009;69:330–4.

[14] Du M, Guo B, Jia D. Newly emerging applications of halloysite nanotubes: A review. Polym Int 2010;59:574–82.

[15] Lvov Y, Abdullayev E. Functional polymer-clay nanotube composites with sustained release of chemical agents. Prog Polym Sci 2013;38:1690–719.

[16] Du M, Guo B, Jia D. Thermal stability and flame retardant effects of halloysite nanotubes on poly(propylene). Eur Polym J 2006;42:1362–9.

[17] Murariu M, Dechief A-L, Paint Y, Peeterbroeck S, Bonnaud L, Dubois P. Polylactide (PLA)—Halloysite Nanocomposites: Production, Morphology and Key-Properties. J Polym Environ 2012;20:932–43.

[18] Carli LN, Crespo JS, Mauler RS. PHBV nanocomposites based on organomodified montmorillonite and halloysite: The effect of clay type on the morphology and thermal and mechanical properties. Compos Part A Appl Sci Manuf 2011;42:1601–8.

[19] Fujii K, Nakagaito AN, Takagi H, Yonekura D. Sulfuric acid treatment of halloysite nanoclay to improve the mechanical properties of PVA/halloysite transparent composite films. Compos Interfaces 2014;21:319–27.

[20] Liu M, Zhang Y, Wu C, Xiong S, Zhou C. Chitosan/halloysite nanotubes bionanocomposites: structure, mechanical properties and biocompatibility. Int J Biol Macromol 2012;51:566–75.

[21] Liu C, Luo Y, Jia Z, Li S, Guo B, Jia D. Structure and Properties of Poly(vinyl chloride)/Halloysite Nanotubes Nanocomposites. J Macromol Sci Part B 2012;51:968–

81.

[22] Ye Y, Chen H, Wu J, Ye L. High impact strength epoxy nanocomposites with natural nanotubes. Polymer (Guildf) 2007;48:6426–33.

[23] Albdiry MTT, Yousif BFF. Morphological structures and tribological performance of unsaturated polyester based untreated/silane-treated halloysite nanotubes. Mater Des 2013;48:68–76.

[24] Vahedi V, Pasbakhsh P. Instrumented impact properties and fracture behaviour of epoxy/modified halloysite nanocomposites. Polym Test 2014;39:101–14.

[25] Ismail H, Pasbakhsh P, Fauzi MNA, Abu Bakar a. Morphological, thermal and tensile properties of halloysite nanotubes filled ethylene propylene diene monomer (EPDM) nanocomposites. Polym Test 2008;27:841–50.

[26] Ismail H, Salleh SZ, Ahmad Z. Properties of halloysite nanotubes-filled natural rubber prepared using different mixing methods. Mater Des 2013;50:790–7.

[27] Prashantha K, Lacrampe M-FF, Krawczak P. Highly dispersed polyamide-11/halloysite nanocomposites: Thermal, rheological, optical, dielectric, and mechanical properties. J Appl Polym Sci 2013;130:313–21.

[28] Rashmi BJ. Toughening of poly(lactic acid) without sacrificing stiffness and strength by melt-blending with polyamide 11 and selective localization of halloysite nanotubes. Express Polym Lett 2015;9:721–35.

[29] Sahnoune M, Taguet A, Otazaghine B, Kaci M, Lopez-Cuesta J-M. Inner surface modification of halloysite nanotubes and its influence on morphology and thermal properties of polystyrene/polyamide-11 blends. Polym Int 2017;66:300–12.

[30] Sahnoune M, Taguet A, Otazaghine B, Kaci M. Effects of functionalized halloysite on morphology and properties of polyamide-11/SEBS-g-MA blends. Eur Polym J 2017;90:418–30.

[31] Kennouche S, Le Moigne N, Kaci M, Quantin JC, Caro-Bretelle AS, Delaite C, et al. Morphological characterization and thermal properties of compatibilized poly(3-hydroxybutyrate-co-3-hydroxyvalerate) (PHBV)/poly(butylene succinate) (PBS)/halloysite ternary nanocomposites. Eur Polym J 2016;75:142–62.

[32] You Y-L, Li D-X, Si G-J, Deng X. Investigation of the influence of solid lubricants on the tribological properties of polyamide 6 nanocomposite. Wear 2014;311:57–64.

[33] Srinath G, Gnanamoorthy R. Sliding wear performance of polyamide 6–clay nanocomposites in water. Compos Sci Technol 2007;67:399–405.

[34] Sun L-H, Yang Z-G, Li X-H. Mechanical and tribological properties of polyoxymethylene modified with nanoparticles and solid lubricants. Polym Eng Sci 2008;48:1824–32.

[35] Cai H, Yan F, Xue Q, Liu W. Investigation of tribological properties of Al2O3-polyimide nanocomposites. Polym Test 2003;22:875–82.

[36] Prashantha K, Schmitt H, Lacrampe MF, Krawczak P. Mechanical behaviour and essential work of fracture of halloysite nanotubes filled polyamide 6 nanocomposites. Compos Sci Technol 2011;71:1859–66.

[37] Handge U a., Hedicke-Höchstötter K, Altstädt V. Composites of polyamide 6 and silicate nanotubes of the mineral halloysite: Influence of molecular weight on thermal, mechanical and rheological properties. Polymer (Guildf) 2010;51:2690–9.

[38] Sharif NFA, Mohamad Z, Hassan A, Wahit MU. Novel epoxidized natural rubber toughened polyamide 6/halloysite nanotubes nanocomposites. J Polym Res 2012;19:9749.